Digest Journal of Nanomaterials and Biostructures Vol. 19, No. 4, October-December 2024, p. 1847-1854

Structural studies and *in vitro* cytotoxic activity of dodecylamine passivated palladium sulfide and ruthenium sulfide quantum dots

A. M. Paca[b], M. Singh[c], P. A. Ajibade[a,*]
[a]*School of Chemistry and Physics, University of KwaZulu-Natal, Pietermaritzburg campus, Private Bag X01, Scottsville 3209, South Africa*
[b]*Department of Pure and Applied Chemistry, University of Fort Hare, Private Bag X1314, Alice 5700, South Africa*
[c]*School of Life Sciences, University of KwaZulu-Natal, Westville campus, Private Bag X54001, Durban, 4000, South Africa*

Dodecylamine capped palladium sulfide (PdS-DDA) and ruthenium sulfide (RuS-DDA) nanoparticles were synthesized from bis(piperidinedithiocarbamato)palladium(II) and tris(piperidinedithiocarbamato)ruthenium(III). The optical band gaps were 4.34 eV for PdS-DDA and 3.63 eV for RuS-DDA nanoparticles. The PdS-DDA corresponds to tetragonal-PdS while RuS-DDA have cubic crystalline phase. The PdS-DDA nanoparticles were monodispersed with particle sizes of 3.15-5.63 nm while the RuS-DDA nanoparticles had particle sizes of 1.18-1.75 nm. Anticancer screening revealed PdS-DDA nanoparticles have better cytotoxicity with IC_{50} of 10.02 μg/mL against HEK293 and 38.89 μg/mL against HeLa in comparison to about 90.02 μg/mL for RuS-DDA nanoparticles against both cells.

(Received April 19, 2024; Accepted December 2, 2024)

Keywords: Single-source precursor, Metal sulfide, Nanoparticles, Dodecylamine, Band gap, pXRD

1. Introduction

Metal chalcogenides nanoparticles are of interest as a result of their unique properties [1-4] especially the particles sizes which dictates their physical and chemical properties [5]. The arrangements of surface atoms in these materials regulate other associated chemical reactions and physical behaviours [6]. One major challenge to the development of nanomaterials lies with the control of their particle size, which ultimately control the physical and chemical properties and their potential applications. Metal sulfide exist in different crystalline phases which offers different applications in diverse fields [7, 8]. Although several methods have been explored to prepare metal sulfide quantum dots, the use of metal chalcogenides complexes offers ways to tuned the physical and chemical attributes through variation of the synthetic parameters [9], [10].

Thermolysis of single source precursors method offers an effective synthetic procedure to well-regulated metal chalcogenide nanomaterials. This route avoids the use of volatile and toxic pyrophoric compounds [11]. Variation of parameters such as the capping agent, temperature, precursor concentration and reaction time influences the nanoparticle particle size [12]. The capping agent protects the surface atoms and prevents the nanoparticles from agglomeration thus promoting monodispersity. In addition, it passivate the surfaces of the nanoparticles through non-covalent interactions with surface atoms, like Lewis bases [12, 13]. Organic polymers [14], dendrimers [15], polysaccharides [16], small ligands [17] and surfactants [18] are widely used but the use of high boiling point alkyl amines offers excellent passivation [19-23].

In this study, dodecylamine capped palladium sulfide and ruthenium sulfide nanoparticles were prepared from bis(piperidinedithiocarbamato)palladium(II) and tris(piperidinedithiocarbamato)ruthenium(III) single source precursors. The optical, structural and morphological properties were studied using spectroscopic techniques, powder X-ray diffraction

* Corresponding author: ajibadep@ukzn.ac.za
https://doi.org/10.15251/DJNB.2024.194.1847

(pXRD) patterns and electron microscopy. *In vitro* cytotoxicity of the as-prepared quantum dots was assessed against human embryonic kidney (HEK293) and cervical cancer (HeLa) cell lines.

2. Experimental

2.1. Materials, methods and physical measurements

Dodecylamine (DDA), oleic acid (OA), methanol and n-hexane were obtained from Merck and used as obtained. Bis(piperidinedithiocarbamato)palladium(II) and tris(piperidinedithiocarbamato)ruthenium(III) were synthesized and characterized as reported [20, 21]. Absorption spectra of the nanoparticles were obtained from Perkin Elmer Lambda 25 spectrophotometer. Photoluminescence spectra of the as-prepared nanoparticles were obtained by a Perkin Elmer LS-45 luminescence spectrophotometer (200-800 nm). The excitation wavelength was set at 350 nm. Samples were prepared in chloroform. Powder XRD was used to determine the crystalline phases of the quantum dots. Powder XRD of palladium sulfide and ruthenium sulfide quantum dots were obtained using Bruker D8 advanced diffractometer. On flat steel, samples were loaded and scanned between 5 and 85°. The diffraction peaks at specific 2θ values were compared to the reference codes of the pXRD Joint Committee on Powder Diffraction Standards (JCPDS) and the documented standards in the Inorganic Crystal Structure Database (ICSD). JEOL HRTEM-2100 electron microscope was utilized to capture the morphological micrograph. ZEISS EVO LS 15 was used to obtained the scanning electron microscopy (SEM) images and electron dispersive X-ray spectroscopy (EDS) spectra. FTIR spectra of the dodecylamine capping agent and the as-prepared nanoparticles were recorded as potassium bromide (KBr) disk using Cary 630 FTIR spectrometer. Anticancer potential of the as-synthesized quantum dots was evaluated using the 3-(4,5-dimethylthiazol-2-yl)-2,5-diphenyltetrazolium bromide (MTT) assay [22]. GraphPad Prism software was used to calculate the IC_{50} values for each experiment, which were carried out in triplicate [23].

2.2. Synthesis of the nanoparticles

Thermal decomposition of single-source precursor (SSP) approach was adopted for the preparation of the palladium sulfide and ruthenium sulfide nanoparticles [24-26]. 0.1 g of each precursor in 2 mL oleic acid (OA) was added to 2 g of hot DDA capping agent with rapid stirring. The experiment was stabilised for 1 h at 200 °C, cooled to 60 °C followed by the addition of methanol to precipitate the resultant quantum dots that were then separated using centrifuge. The excess capping agent and dispersant were rinsed off using methanol. The nanoparticles were dried in a fume-hood and denoted as PdS-DDA and RuS-DDA.

3. Results and discussion

3.1. Optical studies

Fig. 1(a) displays the optical absorption spectra of PdS-DDA and RuS-DDA nanoparticles. For PdS-DDA and RuS-DDA the absorptions were found at 246 and 258 nm, respectively. Band gap energy (Eg) was estimated from Tauc plots, Fig. 1(b). PdS-DDA nanoparticles had an Eg of 4.34 eV, while RuS-DDA nanoparticles had an Eg of 3.63 eV. The shift in the energy band gap of the as-synthesized quantum dots in comparison to their bulk materials, is ascribed to quantum confinement effect of PdS-DDA and RuS-DDA due to their small particle sizes [27].

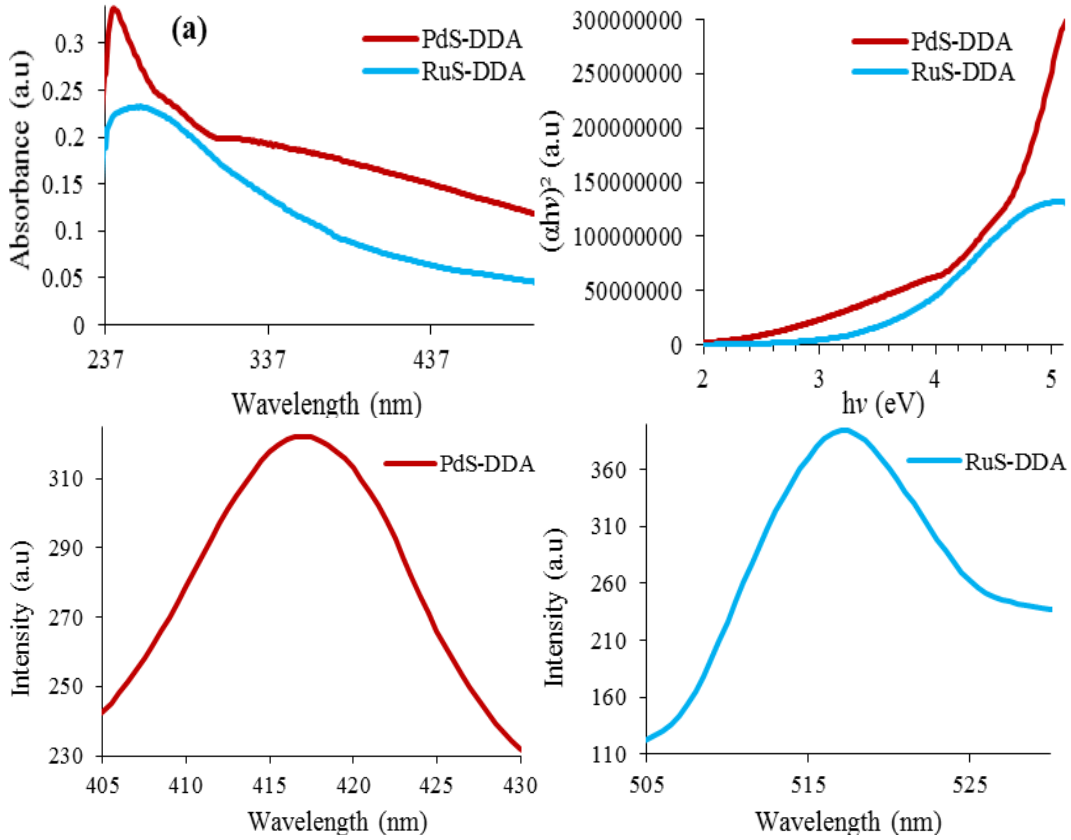

Fig. 1. Absorption spectra (a), Tauc plots (b) and emission spectra (c and d) of PdS-DDA and RuS-DDA quantum dots.

Photoluminescence (PL) spectra of PdS-DDA and RuS-DDA nanoparticles are shown in Fig. 1(c and d). PdS-DDA and RuS-DDA nanoparticles showed emission maxima at 416 and 517 nm, respectively. The size distributions and surface defect states of the as-prepared nanoparticles may be responsible for the broad peaks. The nanoparticles' emission maxima showed a red shift with respect to the band edges of their absorption bands [28].

3.2. Powder X-ray diffraction studies

The pXRD of PdS-DDA quantum dots (Fig. 2) revealed peaks at 22.94, 25.05, 27.18 and 29.14° and were indexed to the (100), (111), (002) and (201) corresponding to the diffraction planes of tetragonal crystalline phase of PdS with data file ICSD: 98-064-8749 [29, 30]. The spectrum for RuS-DDA nanoparticles shows diffraction peaks at 2θ = 27.64, 29.78, 42.25 and 62.62° indexed to (111), (200), (311), (220) and (321). The broadening of diffraction peaks suggests small particle sizes [31]. The pXRD corresponds to cubic crystalline phase of ruthenium sulfide [JCPDS: 00-012-0737] [32, 33]. The (*) are peaks attributed to capping agent.

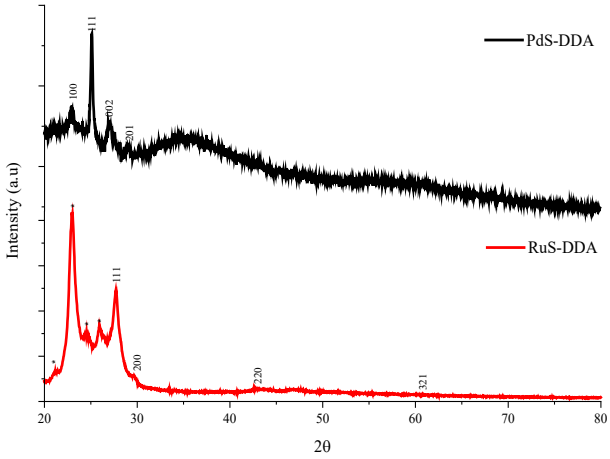

Fig. 2. pXRD of PdS-DDA and RuS-DDA quantum dots capped with dodecylamine.

3.3. HRTEM micrographs of the PdS-DDA and RuS-DDA nanoparticles

HRTEM micrographs of the PdS-DDA nanoparticles' (Fig. 3) displays spherically shaped particles with particle size in the range 3.15 to 5.63 nm. RuS-DDA nanoparticles have particle size in the range 1.18-1.75 nm as tiny dot shaped particles. This indicates that the nature of the precursor influences the nanoparticle particle size. The as-prepared palladium sulfide and ruthenium sulfide nanoparticles could be described as quantum dots because their particles sizes are less than 10 nm. As a result, they can be used for different applications as their large surface-to-volume ratio enables efficient bonding with a lot of other compounds such as biomolecules [34].

Fig. 4 displays the SEM micrographs and EDS spectra of PdS-DDA and RuS-DDA nanoparticles. The SEM image of PdS-DDA shows rough surface flake-like morphology. The nanoparticles have some white patches which is attributed to excess dodecyl amine capping agent. RuS-DDA nanoparticles show rock-like surface morphology with random fibre-like connections. EDS spectrum of PdS-DDA shows palladium and the sulfur while that of RuS-DDA revealed ruthenium and sulfur atoms that confirms successful preparation of palladium sulfide and ruthenium sulfide nanoparticles.

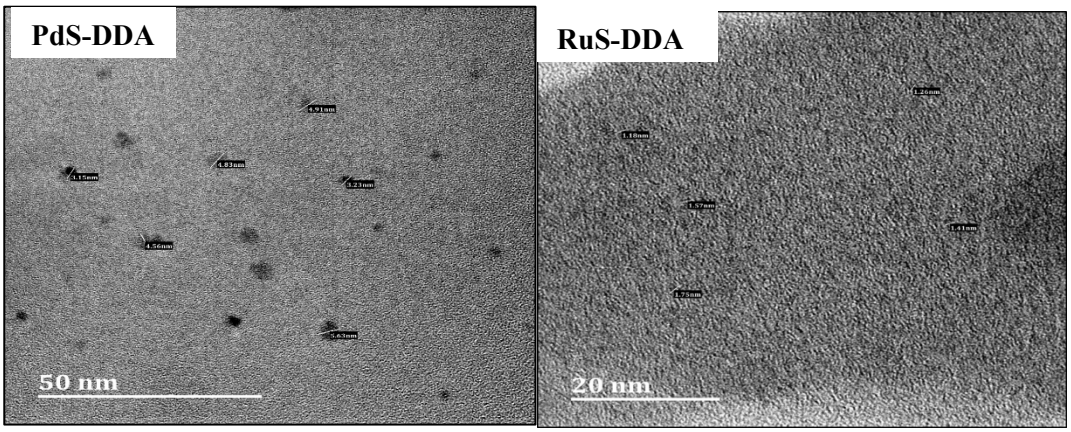

Fig. 3. HRTEM images of PdS-DDA and RuS-DDA quantum dots.

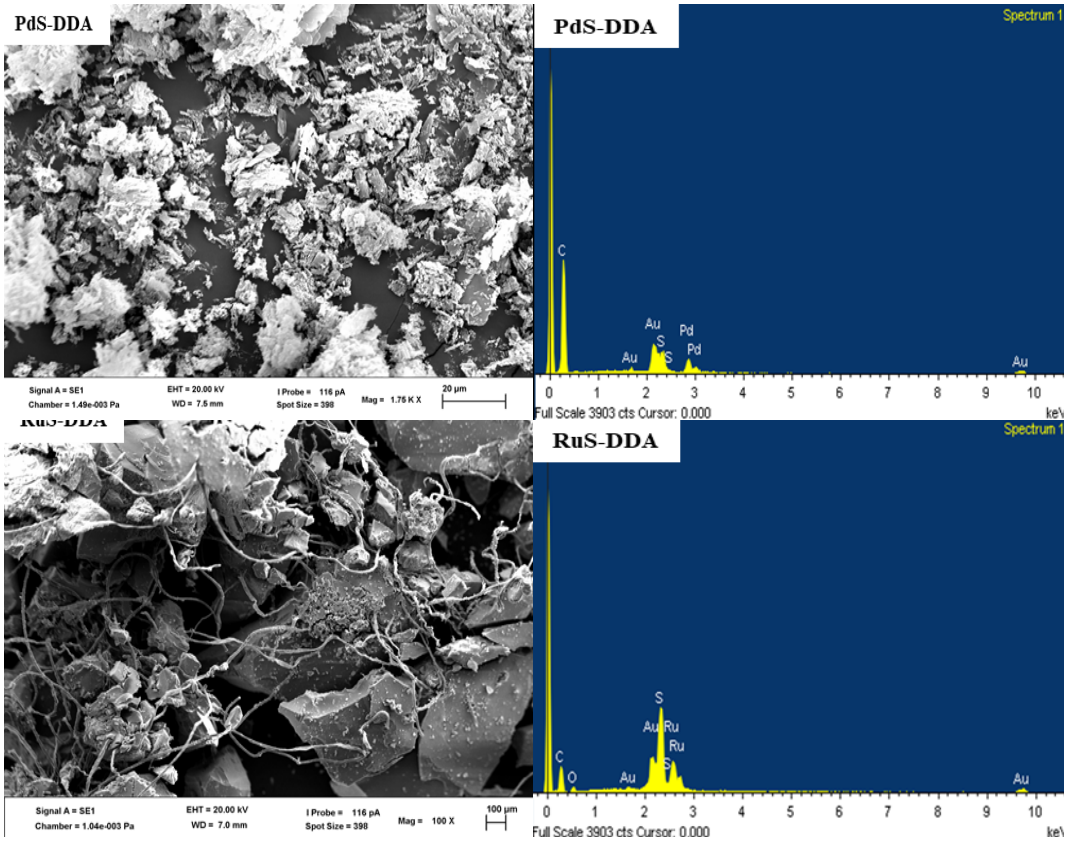

Fig. 4. SEM micrographs and EDS of PdS-DDA and RuS-DDA nanoparticles.

3.4. FTIR studies

FTIR spectra of the docecylamine (DDA), oleic acid (OA), PdS-DDA and RuS-DDA nanoparticles (Fig. 5) shows N–H stretching vibration of DDA appeared at 3330 and 3170 cm^{-1} [35] and the alkyl C–H stretching frequency at 2914 and 2845 cm^{-1} [36]. FTIR spectra of PdS-DDA and RuS-DDA nanoparticles are similar to that of DDA which confirms the stabilization of the nanoparticles by DDA. The OA FTIR revealed prominent stretching frequency at 1705 cm^{-1} that does not appear on the PdS-DDA and RuS-DDA spectra, suggesting that OA did not cap the nanoparticles [37, 38]

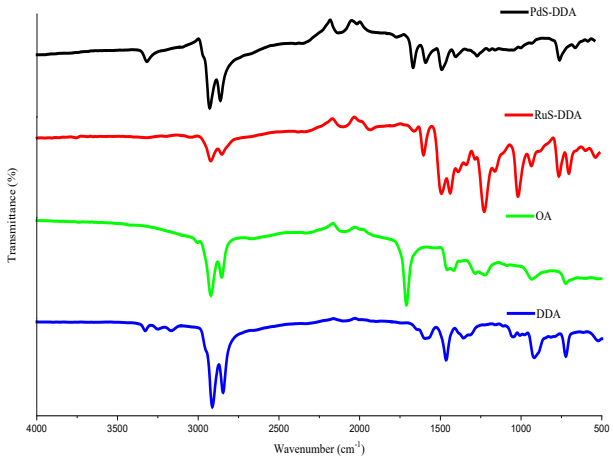

Fig. 5. FTIR of dispersant (OA), capping agent (DDA) and DDA capped palladium sulfide nanoparticle.

3.5. Cytotoxic studies

In vitro cytotoxicity on normal (HEK293) and cancerous (HeLa) human cell lines (Table 1) of the PdS-DDA and RuS-DDA quantum dots indicates that the PdS-DDA is more active than the RuS-DDA. PdS-DDA nanoparticles showed some cytotoxicity in both tested cell lines and even higher cytotoxicity in the normal cells. However, RuS-DDA showed very low cytotoxicity against both cell lines. Both, PdS-DDA and RuS-DDA showed better cytotoxicity in normal cell lines than in cancerous cell lines which mean they lack selectivity.

Table 1. Cytotoxic evaluation of the compounds.

Compounds	IC_{50} (µg/mL)	
	HEK293	HeLa
PdS-DDA	10.02	38.89
RuS-DDA	86.28	92.95

4. Conclusion

We present the synthesis, morphological, optical, and structural properties of PdS-DDA and RuS-DDA nanoparticles capped with dodecylamine. The PdS-DDA nanoparticles have energy bandgap of 4.34 eV and RuS-DDA have an energy bandgap of 3.63 eV. HRTEM micrographs revealed an average particle size of 4.33nm for PdS-DDA nanoparticles and 1.43 nm for RuS-DDA nanoparticles while the SEM images showed different surface morphology for the as-prepared nanoparticles. This demonstrated that the single source chalcogenide precursors utilized to prepare the nanoparticles had an impact on how the nanoparticles formed. FTIR spectra of the palladium sulfide and ruthenium sulfide nanoparticles confirmed the capping with the dodecylamine capping agent. *In vitro* anticancer screening showed that the PdS-DDA nanoparticles have better cytotoxicity with IC_{50} of 10.02 µg/mL against HEK293 and 38.89 µg/mL against HeLa in comparison to 86.28 µg/mL and 92.95 µg/mL for the RuS-DDA nanoparticles against HEK293 and HeLa cells. However, the cytotoxicity is much higher in normal cells (HEK293) than in cancerous cells (HeLa) suggesting that the nanoparticles lack selectivity.

Acknowledgements

The research was supported by NRF South Africa through grant 129275.

References

[1] K. Chen, C. Wang, Z. Peng, K. Qi, Z. Guo, Y. Zhang, H. Zhang, Coord. Chem. Rev. 418, (2020) 1; https://doi.org/10.1016/j.ccr.2020.213333

[2] A. S. Jatoi, F. Akhter, N. M. Mubarak, S. A. Mazari, S. Ahmed, N. Sabzoi, A. Q. Memon, H. A. Baloch, R. Abro, A. Muhammad, Sustainable Nanotechnol. Environ. Rem. (2022) 91; https://doi.org/10.1016/B978-0-12-824547-7.00001-1

[3] Z. Cheng, T. Zhao, H. Zeng, Small Sci. 2, (2022) 2100051; https://doi.org/10.1002/smsc.202100051

[4] J. Zhou, Z. Liu, X. Liu, G. Fu, G. Liu, J. Chen, C. Wang, H. Zhang, M. Hong, J. Mater. Chem. C 8 (2020) 12768; https://doi.org/10.1039/D0TC01990A

[5] S. C. Subbenaik. Physical and chemical nature of nanoparticles. In Plant nanotechnology, Springer, 2016; pp 15-27; https://doi.org/10.1007/978-3-319-42154-4_2

[6] M. K. Nayak, J. Singh, B. Singh, S. Soni, V. S. Pandey, S. Tyagi. Introduction to semiconductor nanomaterial and its optical and electronics properties. In Metal Semiconductor Core-Shell Nanostructures for Energy and Environmental Applications, Elsevier, 2017; pp 1-33; https://doi.org/10.1016/B978-0-323-44922-9.00001-6

[7] A. Gaiardo, B. Fabbri, V. Guidi, P. Bellutti, A. Giberti, S. Gherardi, L. Vanzetti, C. Malagù, G. Zonta, Sensors 16 (2016) 1-19; https://doi.org/10.3390/s16030296

[8] T. W. Mammo, N. Murali, C. V. Kumari, S. Margarette, A. Ramakrishna, R. Vemuri, Y. S. Rao, K. V. Prasad, Y. Ramakrishna, K. Samatha, Phys. B: Condens. Matter 581 (2020) 411769; https://doi.org/10.1016/j.physb.2019.411769

[9] C. Rao, S. Vivekchand, K. Biswas, A. Govindaraj, Dalton Trans (2007) 3728; https://doi.org/10.1039/b708342d

[10] J. Z. Mbese, P. A. Ajibade. J. Sulfur Chem., (2014) 35(4), 438; https://doi.org/10.1080/17415993.2014.912280

[11] Y. C. Zhang, W. W. Chen, X. Y. Hu, Cryst. Growth Des. 7 (2007) 580; https://doi.org/10.1021/cg060597f

[12] B. K. Sodipo, O. A. Noqta, A. A. Aziz, M. Katsikini, F. Pinakidou, E. C. Paloura, J. Alloys Compd. 938 (2023) 168558; https://doi.org/10.1016/j.jallcom.2022.168558

[13] S. Pedroso-Santana, N. Fleitas-Salazar, Part. Part. Syst. Char. 40 (2023) 2200146; https://doi.org/10.1002/ppsc.202200146

[14] S. Campisi, M. Schiavoni, C. E. Chan-Thaw, A. Villa, Catalysts 6 (2016) 1; https://doi.org/10.3390/catal6120185

[15] L. Kannappan, R. Rajmohan, P. Edwin, Mater. Lett. 301 (2021) 130257; https://doi.org/10.1016/j.matlet.2021.130257

[16] P. Raveendran, J. Fu, S. L. Wallen, J. Am. Chem. Soc. 125 (2003) 13940; https://doi.org/10.1021/ja029267j

[17] D. J. Gavia, Y. S. Shon, Chem. Cat. Chem. 7 (2015) 892; https://doi.org/10.1002/cctc.201402865

[18] D. K. Smith, B. A. Korgel, Langmuir 24 (2008) 644; https://doi.org/10.1021/la703625a

[19] R. Abargues, J. Navarro, P. J. Rodríguez-Cantó, A. Maulu, J. F. Sánchez-Royo, J. P. Martínez-Pastor, Nanoscale 11 (2019) 1978; https://doi.org/10.1039/C8NR07760F

[20] A. M. Paca, P. A. Ajibade, F. P. Andrew, N. Nundkumar, M. Singh, Arabian J. Chem. 14 (2021) 1; https://doi.org/10.1016/j.arabjc.2021.103326

[21] A. M. Paca, P. A. Ajibade, J. Mol. Struct. 1243 (2021) 130777; https://doi.org/10.1016/j.molstruc.2021.130777

[22] P. A. Ajibade, T. B. Mbuyazi, A. M. Paca, F. P. Andrew, M. Singh, J. Mol. Struct. 1312 (2024) 138357; https://doi.org/10.1016/j.molstruc.2024.138537

[23] D. Montagner, C. Marzano, V. Gandin, Inorg. Chim. Acta 376 (2011) 574; https://doi.org/10.1016/j.ica.2011.07.031

[24] N. L. Botha, P. A. Ajibade, Opt. Quantum Electron. 52 (2020) 1; https://doi.org/10.1007/s11082-020-02455-w

[25] J. Z. Mbese, P. A. Ajibade, J. Sulfur Chem. 38 (2017) 173; https://doi.org/10.1080/17415993.2016.1262373

[26] S. Sibokoza, M. Moloto, N. Moloto, P. Sibiya, Chalcogenide Lett. 14 (2017) 69.

[27] J. Z. Mbese, P. A. Ajibade, J. Mol. Struct. 1143 (2017) 274; https://doi.org/10.1016/j.molstruc.2017.04.095

[28] Z. Zhang, W. P. Lim, C. T. Wong, H. Xu, F. Yin, W. S. Chin, Nanomaterials 2,(2012) 113; https://doi.org/10.3390/nano2020113

[29] M. Barawi, I. Ferrer, J. Ares, C. Sánchez, ACS Appl. Mater. Interfaces 6 (2014) 20544; https://doi.org/10.1021/am5061504

[30] M. A. Ehsan, H. N. Ming, V. McKee, T. A. N. Peiris, U. Wijayantha-Kahagala-Gamage, Z. Arifin, M. Mazhar, New J. Chem. 38 (2014) 4083; https://doi.org/10.1039/C4NJ00564C

[31] R. Bolagam, S. Um, Electrochim. Acta 281 (2018) 571; https://doi.org/10.1016/j.electacta.2018.06.004

[32] S. Kubendhiran, R. Sakthivel, S.-M. Chen, R. Anbazhagan, H.-C. Tsai, Compos. B. Eng. 168 (2019) 282; https://doi.org/10.1016/j.compositesb.2018.12.082

[33] A. Sangili, R. Sakthivel, S. M. Chen, Anal. Chim. Acta 1131 (2020) 35; https://doi.org/10.1016/j.aca.2020.07.032

[34] N. Narayan, A. Meiyazhagan, R. Vajtai, Metal nanoparticles as green catalysts, Materials 12 (2019) 3602; https://doi.org/10.3390/ma12213602

[35] J. Ferlay, M. Colombet, I. Soerjomataram, D. M. Parkin, M. Piñeros, A. Znaor, F. Bray, Int. J. Cancer 149 (2021) 778; https://doi.org/10.1002/ijc.33588

[36] S. Khurshid, Z. Gul, J. Khatoon, M. R. Shah, I. Hamid, I. A. T. Khan, F. Aslam, RSC Adv. 10 (2020) 1021; https://doi.org/10.1039/C9RA07686G

[37] L. Polavarapu, N. Venkatram, W. Ji, Q.-H. Xu, ACS Appl. Mater. Inter. 1, (2009) 2298; https://doi.org/10.1021/am900442u

[38] P. F. Hsiao, S. Peng, T.-C. Tang, S.-Y. Lin, H.-C. Tsai, Int. J. Nanomed. 11 (2016) 1867.